Pressure-induced isostructural transition in a distorted perovskite via octahedron reconfiguration

Fang Hong, Binbin Yue, Naohisa Hirao, Guohao Ren, Bin Chen, and Ho-Kwang Mao

Citation: Appl. Phys. Lett. **109**, 241904 (2016); doi: 10.1063/1.4972303
View online: http://dx.doi.org/10.1063/1.4972303
View Table of Contents: http://aip.scitation.org/toc/apl/109/24
Published by the American Institute of Physics

Pressure-induced isostructural transition in a distorted perovskite via octahedron reconfiguration

Fang Hong,[1,2] Binbin Yue,[1,2,a)] Naohisa Hirao,[3] Guohao Ren,[4] Bin Chen,[1,a)] and Ho-Kwang Mao[1,5]

[1]*Center for High Pressure Science and Technology Advanced Research, 1690 Cailun Rd. Pudong, Shanghai 201203, People's Republic of China*
[2]*The Advanced Light Source, Lawrence Berkeley National Laboratory, 1 Cyclotron Rd, Berkeley, California 94720, USA*
[3]*SPring-8/JASRI, 1-1-1 Kouto, Sayo-cho, Sayo-gun, Hyogo 679-5198, Japan*
[4]*Shanghai Institute of Ceramics, Chinese Academy of Sciences, No. 215 Chengbei Road, Jiading District, Shanghai 201800, People's Republic of China*
[5]*Geophysical Laboratory, Carnegie Institution of Washington, Washington, DC 20015, USA*

(Received 9 September 2016; accepted 26 November 2016; published online 16 December 2016)

Perovskite material studies encompass many fields such as energy harvesting, superconductivity, magnetism, and beyond. Thus, it is very important to investigate their structural varieties in external environments. Here, the pressure-induced structure change of a distorted perovskite, $Y_{0.7}Lu_{0.3}AlO_3$, was examined by synchrotron x-ray diffraction. Upon compression, it underwent an isostructural transition near 22 GPa. The quenchable high-pressure phase had a much higher bulk modulus than the low-pressure phase. This work shows the flexibility of perovskite distortion and will help to understand the property anomalies in prevailing perovskite ABO_3 systems and design more functional materials. *Published by AIP Publishing.* [http://dx.doi.org/10.1063/1.4972303]

Numerous natural minerals and artificial materials form in a perovskite (ABX_3) structure.[1–4] Perovskite-type materials have many interesting properties and applications including the abundant magnetic behaviors of $LAMnO_3$ (LA: lanthanide elements),[5–11] the superconductive behavior of non-oxide $MgCNi_3$,[12] and the promising applications of multiferroic $DyMnO_3$ and $TbMnO_3$ in spintronic devices and high-density information storage.[6,13–15] Perovskite material-based solar cells have also shown excellent energy harvesting performance.[16,17] Hence, studying perovskite materials benefits both fundamental research and industrial applications.

Perovskite ABX_3 compounds have various structures due to the flexibility of their octahedral BX_6 units. The two most common phases are cubic and orthorhombic. $SrTiO_3$ is a typical cubic perovskite compound at room temperature,[18] while $CaTiO_3$ has an orthorhombic structure.[19] $CaTiO_3$ has high-temperature tetragonal and cubic phases near 1500 and 1630 K, respectively.[19] Most magnetic $LAMnO_3$ and $LAFeO_3$ compounds[5,9,20,21] and non-magnetic $LAAlO_3$ compounds[22,23] are orthorhombic phases at ambient conditions. The atomic sizes of their LA elements and B-site elements affect their structure by distorting the octahedral BO_6 units. Therefore, the magnetic behaviors of $LaMnO_3$, $NdMnO_3$, and $DyMnO_3$ are quite different from each other.[5,7,9,11,24] Due to the instability introduced by distortion, $YMnO_3$ is a hexagonal phase at ambient conditions.[25] However, if Al replaces B-site Mn or Fe, it stabilizes $YAlO_3$ and Lu-doped $YAlO_3$ in an orthorhombic but strongly distorted perovskite phase.

Generally, material structures directly relate to physical and chemical properties. Structural studies of perovskite materials under chemical and physical pressure help to reveal distortion evolution, which provides clues for understanding their physical/chemical properties and abnormal behavior. This consequently benefits material design.[8,9,24,26,27] Based on this motivation, we investigated the structure of a distorted perovskite, $Y_{0.7}Lu_{0.3}AlO_3$, under pressure using synchrotron X-ray microdiffraction. We observed an unexpected isostructural transition near 22 GPa and the high-pressure phase (HPP) showed a much higher bulk modulus than the low-pressure phase (LPP). Unlike previous isostructural transitions that accompanied a large volume collapse, there was no significant volume collapse near the transition pressure and the quenchable high-pressure phase had an even larger volume in the low-pressure range.

The $Y_{0.7}Lu_{0.3}AlO_3$ sample was synthesized by a solid-state reaction method, using high-purity raw starting materials Y_2O_3, Lu_2O_3, and Al_2O_3 from Sigma-Aldrich (calcined at 1000 °C for 3 h first and then sintered at 1400 °C for 48 h in a tube furnace with slow air flow). *In situ* X-ray diffraction (XRD) patterns under various pressures were collected from the $Y_{0.7}Lu_{0.3}AlO_3$ sample, which was loaded into a Mao-type symmetric diamond anvil cell (DAC) with a diamond culet of 300 μm. Silicone oil was used as a pressure-transmitting medium and pressure was monitored by the Ruby R1-R2 line shift. We used a stainless steel gasket and laser-drilled a 100 μm sample hole. The *in situ* synchrotron micro X-ray diffraction experiment was carried out at Beamline 10XU in Spring-8; the incident X-ray wavelength was 0.4142 Å and the beam size was 25×35 μm. A fine CeO_2 powder sample was used to calibrate our experimental parameters. The patterns were collected by a Perkin Elmer digital x-ray flat panel detector and the experiment was conducted at room temperature. Lattice structure refinement was performed with *MAUD* software.

At ambient conditions, $Y_{0.7}Lu_{0.3}AlO_3$ has an orthorhombic structure with space group *Pbnm*. Figure 1(a) displays the

a)Electronic addresses: yuebb@hpstar.ac.cn and chenbin@hpstar.ac.cn

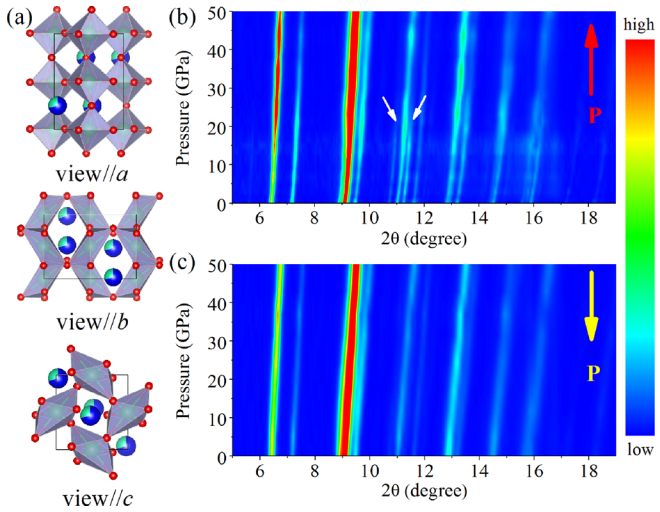

FIG. 1. The atomic structure of as-grown $Y_{0.7}Lu_{0.3}AlO_3$ at ambient conditions and its pressure-dependent two-dimensional X-ray diffraction patterns. (a) The atomic structure of $Y_{0.7}Lu_{0.3}AlO_3$ (Large atom: Y/Lu; Medium atom: Al (inside the cage); Small atom: O); (b) XRD patterns collected during compression; (c) XRD patterns collected during decompression.

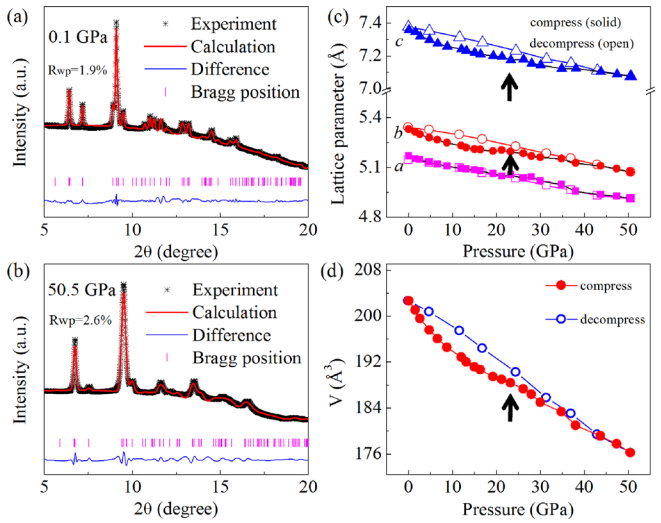

FIG. 2. The representative refinement patterns and the pressure-dependent lattice parameters and unit cell volumes. (a) and (b) The refinement patterns for 0.1 and 50.5 GPa, respectively; (c) pressure-dependent lattice parameters; (d) volume evolution under high pressure (solid: compression; open: decompression). The minor kink near 22 GPa indicates a possible isostructural phase transition.

atomic structure of the unit cell viewed from the *a*, *b*, and *c* axes, respectively. Unlike orthoferrite $LaFeO_3$, the octahedral AlO_6 units in $Y_{0.7}Lu_{0.3}AlO_3$ were strongly distorted both in-plane (IP) and out-of-plane;[28] most significantly along the *b* and *c* axes. To study $Y_{0.7}Lu_{0.3}AlO_3$ structural variety under high pressure, we used synchrotron X-ray diffraction (XRD) to examine its lattice structure. Figure 1(b) displays the XRD pattern collected at ambient conditions to ~50 GPa, while Figure 1(c) demonstrates the XRD patterns collected during decompression. We noticed some changes in peak intensity with pressure, especially in the first two peaks. The intensity of the second peak greatly reduced under increasing pressure. Meanwhile, the two peaks indicated by white arrows near 11° were strongly suppressed by pressure and became very weak above ~22 GPa. Below this pressure, all peaks showed a curvature compression behavior. In contrast, they showed a quasi-linear compression behavior above ~22 GPa. Beyond these changes, no extra diffraction peaks appeared, which could signify an isostructural transition. Though broadening of the measured X-ray diffraction peaks indicates the presence of non-hydrostatic conditions at high pressure, this does not seem to have an effect on the observed isostructural transition described here.

We investigated this structural evolution under high pressure based on the Rietveld refinements of all patterns using the *Pbnm* space group. Figures 2(a) and 2(b) show two representative refinement patterns: (a) shows the refinement pattern at 0.1 GPa and (b) shows the refinement pattern at 50.5 GPa. The pressure-dependent lattice parameters and volumes are presented in Figures 2(c) and 2(d), respectively. All lattice parameters show a monotonously decreasing trend upon compression. Interestingly, both the *b* and *c* axes clearly show abnormal behavior around 22 GPa during compression, compared with decompression, as indicated by the arrows. We also observed this trend change in the pressure-dependent volumes. The different pressure dependence of the lattice parameters and volumes during compression and decompression confirms the occurrence of an isostructural transition. Hence, the low-pressure phase (LPP) exists up to ~22 GPa. Above this pressure, the sample starts to transform to a high-pressure phase (HPP) and the transition appears to finish near 42 GPa, according to the pressure-dependent lattice parameters and volume trend. The HPP remains stable at ~50.5 GPa, our current experimental limit. When pressure decreases from the highest pressure, the HPP remains, even when pressure is fully released. Furthermore, the LPP and HPP show different compressibility.

To understand the pressure effect on the octahedral AlO_6 units' distortion, we extracted information about the related bond angle and bond length from our refinement results. To avoid misunderstanding, we will only discuss the information from the pure LPP and HPP, as shown in Figures 3 and 4,

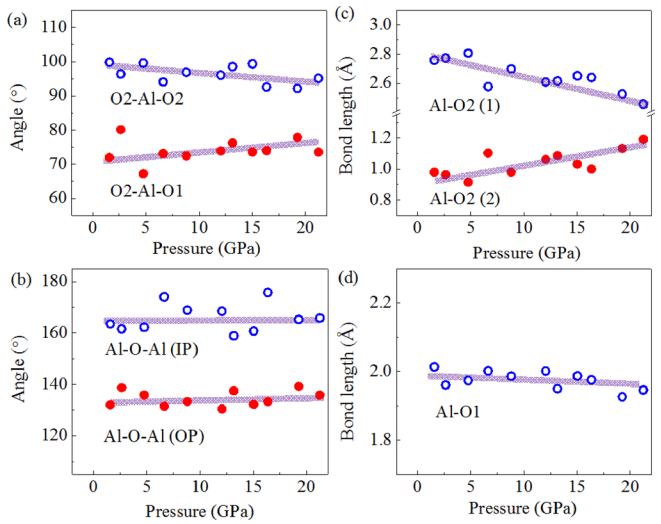

FIG. 3. The pressure-dependent bond lengths and bond angles of the low-pressure phase (LPP), obtained under compression. (a) The O-Al-O bond angles inside the octahedral AlO_6 units; (b) the Al-O-Al bond angles between the octahedral AlO_6 units; (c) the bond lengths of Al-O2 (AlO_4 plane); and (d) the bond lengths of Al-O1.

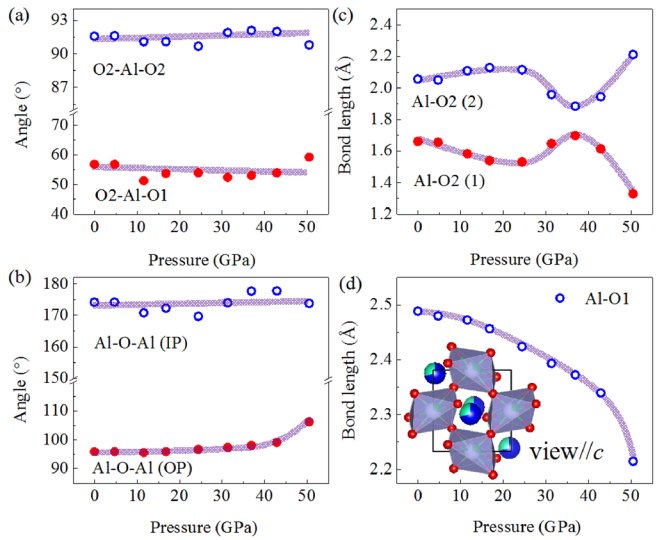

FIG. 4. The pressure-dependent bond lengths and bond angles of the high-pressure phase (HPP) obtained from decompression. (a) The O-Al-O bond angles inside the octahedral AlO_6 units; (b) the Al-O-Al bond angles between the octahedral AlO_6 units; (c) the bond lengths of Al-O2 (AlO_4 plane); and (d) the bond lengths of Al-O1 (inset: the HPP atomic structure at ambient conditions, viewing // *c* axis).

respectively. The bond angles (shown in Figures 3(a) and 3(b)) and bond lengths (shown in Figures 3(c) and 3(d)) of the LPP obtained under compression fluctuate to some extent. This is induced by refinement disturbance from some relatively big grains, which affect the intensity of some peaks. Obtaining a fine powder by physically grinding this material is difficult because its Mohs hardness is around 8.6, which is comparable to corundum.[29] Despite the fluctuation, we can still see an approximate trend, guided by the solid purple line. The in-plane (IP) O2-Al-O2 bond angle becomes smaller when pressure increases, while the out-of-plane (OP) O2-Al-O1 bond angle increases under compression. Interestingly, the synergistic move of both these bond angles towards 90° suggests that the octahedral AlO_6 units distort less under compression. Meanwhile, the in-plane Al-O bond lengths display a similar trend, as shown in Figure 3(c). This pushes the distorted octahedral AlO_6 unit further towards an ideal octahedral structure. The IP and OP Al-O-Al bond angles reflect the relative arrangement of the octahedral AlO_6 units and only show weak pressure dependence. The Al-O1 bond length relates to the compressibility of the *c* axis to some extent and it displays a declining trend upon compression. Therefore, we found that compression drives the distorted octahedral AlO_6 units towards a less distorted structure, while the relative arrangement of the octahedral AlO_6 unit does not change significantly, and the octahedral AlO_6 unit shrinks along the *c* axis.

During decompression, the bond angles and bond lengths give more information about the dynamic movement of the octahedral AlO_6 units, as shown in Figure 4, along with information about the pressure effect on the HPP. When pressure releases, the in-plane and out-of-plane O-Al-O bond angles and the in-plane Al-O-Al bond angle all display weak pressure dependence (Figure 4(a)). The out-of-plane Al-O-Al bond angle given in Figure 4(b) shows weak positive pressure dependence and reduces, suggesting that distortion increases as pressure decreases. The trends of the pressure-dependent in-plane Al-O bond lengths displayed in Figure 4(c) show mirror-like symmetry around 1.82 Å. There is an obvious renormalization of the octahedral AlO_6 units near 38 GPa. Above this pressure, the two in-plane Al-O bond lengths change sharply and the out-of-plane Al-O bond length also markedly contracts, as shown in Figure 4(d). The pressure-dependent out-of-plane Al-O-Al behaves similarly. We noticed that the bond lengths and bond angles in the high-pressure phase differ significantly to those in the low-pressure phase. Compared with the LPP, the octahedral AlO_6 unit extends along the *c* axis in the HPP and the difference between the two in-plane Al-O bond lengths is smaller. Our Figure 4(d) inset shows the HPP atomic structure, viewed along the *c* axis.

We studied the compressibility of the LPP and HPP by Birch-Murnaghan equation of state (EOS) analysis,[30,31] shown in Figure 5. Considering the similarity between $YAlO_3$ and $Y_{0.7}Lu_{0.3}AlO_3$, we used $K' = 7.3$ from a previous study on a single crystal $YAlO_3$ for the LPP of $Y_{0.7}Lu_{0.3}AlO_3$; this gave the bulk modulus $K = 203.9$ GPa, which is very similar to single crystal $YAlO_3$ (~192 GPa).[32] For the HPP, we fixed $K' = 1$, giving the bulk modulus $K = 336.2$ GPa. The V_0 values of these two phases are almost identical, around 203 Å^3. Clearly, the HPP has a much higher bulk modulus than the LPP. This different compressibility behavior stems from their different octahedral AlO_6 unit configuration. When K' and V_0 are free to refine, we obtain a much better fitting and the bulk modulus difference between the two phases grows: for the LPP, $V_0 = 202.6 \pm 1$ Å^3, $K = 156.2 \pm 58.9$ GPa, and $K' = 18.6 \pm 13.13$; for the HPP, $V_0 = 203.3 \pm 0.43$ Å^3, $K = 359.0 \pm 23.1$ GPa, and $K' = 0.33 \pm 0.62$. It should be noted that the LPP shows a clear curvature compression behavior and a large K' value was obtained (the K' value is still smaller than those of Mo and Ni[33]). On the contrary, the HPP shows a quasi-linear compression behavior and a small K' value was obtained consequently. Small K' values were also found in stishovite SiO_2 ($K' = 1.7 \pm 0.6$ in Ross's work,[34] $K' = 0.7 \pm 1.1$ in Sato's work[35]) and cotunnite-type TiO_2 ($K' = 1.35 \pm 0.1$).[36] Hence, the configuration of the octahedral AlO_6 units determines the structural properties of perovskite materials, which could further affect their electronic, optical, and other physical properties.

An isostructural transition occurs in various material systems and sometimes it changes their physical properties significantly.[37–39] Usually, an isostructural transition accompanies a volume collapse;[38,40] for example, there is a 9.8% volume collapse during the isostructural transition in cubic perovskite $PbCrO_3$, an important natural mineral.[38] The size

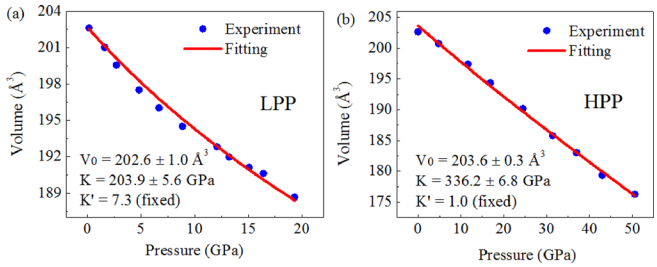

FIG. 5. Birch-Murnaghan equation of state (EOS) analysis. (a) EOS analysis for the LPP; and (b) EOS analysis for the HPP.

of volume collapse during the isostructural transition in samarium compounds can also reach 6%–9%.[41] However, we did not observe any significant volume collapse near the transition pressure of our perovskite. On the contrary, in the low-pressure range (5–22 GPa, shown in Figure 2(d)) the HPP has a larger volume than the original LPP. Furthermore, most isostructural transitions originate from electronic transitions or spin state transitions.[39,40,42,43] The isostructural transition in pure cerium is caused by the delocalization of the localized f-electron[43] and the isostructural transitions in orthorhombic $RFeO_3$ are induced by a spin state transition.[40] In our work, there was no transition metal element and the electronic structure of Al^{3+} remained very stable because all of the 2s2p orbitals were fully occupied so they could not undergo an electronic transition. Similarly, no electronic transition occurred in Y^{3+} and Lu^{3+} because all their orbitals in the outermost occupied shells were also fully occupied. Therefore, the isostructural transition in $Y_{0.7}Lu_{0.3}AlO_3$ is not caused by an electronic transition but by the reconfiguration of the octahedral AlO_6 units and is completely structural in origin.

In summary, we observed a pressure-induced isostructural transition in the distorted perovskite $Y_{0.7}Lu_{0.3}AlO_3$ using synchrotron X-ray microdiffraction. We found curvature compression behavior in the low-pressure phase (LPP) but quasi-linear compression behavior in the high-pressure phase (HPP). The HPP was maintained under full pressure release. The change of flexibility in the octahedral AlO_6 units favored the isostructural HPP rather than a symmetry change. The HPP had a bulk modulus ~336 GPa, much higher than (~204 GPa) the low-pressure phase. In addition, there was no electronic transition, spin state transition, or volume collapse during the isostructural transition. On the contrary, the HPP had a larger volume than the LPP in the low-pressure range. This work demonstrates that the octahedral AlO_6 unit configuration has a strong effect on the $Y_{0.7}Lu_{0.3}AlO_3$ structural properties and furthers our understanding of the complex physical behaviors of various perovskite materials.

The authors acknowledge support from the NSAF (Grant No. U1530402). F.H. and B.B.Y. acknowledge the usage of beam time at Beamline 10XU in Spring-8 (PN: 2014B1254). All authors thank Freyja O'Toole for her careful revision of the manuscript.

[1]N. Tomioka and K. Fujino, Science **277**, 1084–1086 (1997).
[2]M. Miyahara, E. Ohtani, S. Ozawa, M. Kimura, A. El Goresy, T. Sakai, T. Nagase, K. Hiraga, N. Hirao, and Y. Ohishi, Proc. Natl. Acad. Sci. U.S.A. **108**, 5999–6003 (2011).
[3]A. V. Kimel, A. Kirilyuk, A. Tsvetkov, R. V. Pisarev, and T. Rasing, Nature **429**, 850–853 (2004).
[4]Y. Tokunaga, S. Iguchi, T. Arima, and Y. Tokura, Phys. Rev. Lett. **101**, 097205 (2008).
[5]I. Solovyev, N. Hamada, and K. Terakura, Phys. Rev. Lett. **76**, 4825–4828 (1996).
[6]O. Prokhnenko, R. Feyerherm, E. Dudzik, S. Landsgesell, N. Aliouane, L. C. Chapon, and D. N. Argyriou, Phys. Rev. Lett. **98**, 057206 (2007).
[7]C. Wehrenfennig, D. Meier, T. Lottermoser, T. Lonkai, J. U. Hoffmann, N. Aliouane, D. N. Argyriou, and M. Fiebig, Phys. Rev. B **82**, 100414 (2010).
[8]J. Hemberger, S. Lobina, H. A. K. von Nidda, N. Tristan, V. Y. Ivanov, A. A. Mukhin, A. M. Balbashov, and A. Loidl, Phys. Rev. B **70**, 024414 (2004).
[9]F. Hong, Z. Cheng, and X. Wang, Appl. Phys. Lett. **99**, 192503 (2011).
[10]F. Hong, Z. Cheng, H. Zhao, H. Kimura, and X. Wang, Appl. Phys. Lett. **99**, 092502 (2011).
[11]F. Hong, Z. Cheng, J. Wang, X. Wang, and S. Dou, Appl. Phys. Lett. **101**, 102411 (2012).
[12]T. He, Q. Huang, A. P. Ramirez, Y. Wang, K. A. Regan, N. Rogado, M. A. Hayward, M. K. Haas, J. S. Slusky, K. Inumara, H. W. Zandbergen, N. P. Ong, and R. J. Cava, Nature **411**, 54–56 (2001).
[13]T. Kimura, G. Lawes, T. Goto, Y. Tokura, and A. P. Ramirez, Phys. Rev. B **71**, 224425 (2005).
[14]M. Mostovoy, Phys. Rev. Lett. **96**, 067601 (2006).
[15]M. Matsubara, S. Manz, M. Mochizuki, T. Kubacka, A. Iyama, N. Aliouane, T. Kimura, S. L. Johnson, D. Meier, and M. Fiebig, Science **348**, 1112–1115 (2015).
[16]M. Liu, M. B. Johnston, and H. J. Snaith, Nature **501**, 395–398 (2013).
[17]W.-J. Yin, T. Shi, and Y. Yan, Appl. Phys. Lett. **104**, 063903 (2014).
[18]R. Loetzsch, A. Lübcke, I. Uschmann, E. Förster, V. Große, M. Thuerk, T. Koettig, F. Schmidl, and P. Seidel, Appl. Phys. Lett. **96**, 071901 (2010).
[19]R. Ali and M. Yashima, J. Solid State Chem. **178**, 2867–2872 (2005).
[20]J. Laverdiere, S. Jandl, A. A. Mukhin, V. Y. Ivanov, V. G. Ivanov, and M. N. Iliev, Phys. Rev. B **73**, 214301 (2006).
[21]R. L. White, J. Appl. Phys. **40**, 1061–1069 (1969).
[22]M. Weber, M. Bass, K. Andringa, R. Monchamp, and E. Comperchio, Appl. Phys. Lett. **15**, 342–345 (1969).
[23]P. Dereń, A. Bednarkiewicz, P. Goldner, and O. Guillot-Noël, J. Appl. Phys. **103**, 043102 (2008).
[24]F. Hong, Z. Cheng, X. Wang, and S. Dou, Appl. Phys. Lett. **101**, 121913 (2012).
[25]H. Lueken, Angew. Chem., Int. Ed. **47**, 8562–8564 (2008).
[26]J. Hemberger, F. Schrettle, A. Pimenov, P. Lunkenheimer, V. Y. Ivanov, A. A. Mukhin, A. M. Balbashov, and A. Loidl, Phys. Rev. B **75**, 035118 (2007).
[27]A. Shireen, R. Saha, P. Mandal, A. Sundaresan, and C. N. R. Rao, J. Mater. Chem. **21**, 57–59 (2011).
[28]S. Geller and E. Wood, Acta Crystallogr. **9**, 563–568 (1956).
[29]M. Fibrich, J. Šulc, H. Jelínková, K. Nejezchleb, and V. Škoda, Laser Phys. Lett. **7**, 290 (2010).
[30]F. D. Murnaghan, Proc. Natl. Acad. Sci. U.S.A. **30**, 244–247 (1944).
[31]F. Birch, Phys. Rev. **71**, 809–824 (1947).
[32]N. Ross, J. Zhao, and R. Angel, J. Solid State Chem. **177**, 1276–1284 (2004).
[33]L. Gerward, J. Phys. Chem. Solids **46**, 925–927 (1985).
[34]N. L. Ross, J. Shu, and R. M. Hazen, Am. Mineral. **75**, 739–747 (1990), see http://www.minsocam.org/ammin/AM75/AM75_739.pdf.
[35]Y. Sato, Earth Planet. Sci. Lett. **34**, 307–312 (1977).
[36]L. S. Dubrovinsky, N. A. Dubrovinskaia, V. Swamy, J. Muscat, N. M. Harrison, R. Ahuja, B. Holm, and B. Johansson, Nature **410**, 653–654 (2001).
[37]C. S. Yoo, B. Maddox, J. H. P. Klepeis, V. Iota, W. Evans, A. McMahan, M. Y. Hu, P. Chow, M. Somayazulu, D. Häusermann, R. T. Scalettar, and W. E. Pickett, Phys. Rev. Lett. **94**, 115502 (2005).
[38]W. Xiao, D. Tan, X. Xiong, J. Liu, and J. Xu, Proc. Natl. Acad. Sci. U.S.A. **107**, 14026–14029 (2010).
[39]S. Wang, J. Zhu, Y. Zhang, X. Yu, J. Zhang, W. Wang, L. Bai, J. Qian, L. Yin, and N. S. Sullivan, Proc. Natl. Acad. Sci. U.S.A. **112**, 15320–15325 (2015).
[40]G. K. Rozenberg, M. Pasternak, W. Xu, L. Dubrovinsky, S. Carlson, and R. Taylor, Europhys. Lett. **71**, 228 (2005).
[41]M. Singh, A. Gour, and S. Singh, Acta Phys. Pol., A **123**, 709–713 (2013).
[42]H. T. Hall, L. Merrill, and J. D. Barnett, Science **146**, 1297–1299 (1964).
[43]M. Lipp, D. Jackson, H. Cynn, C. Aracne, W. Evans, and A. McMahan, Phys. Rev. Lett. **101**, 165703 (2008).